Modulational Instability in Fiber Bragg Grating With Non-Kerr Nonlinearity

K. Porsezian, K. Senthilnathan, and S. Devipriya

***Abstract*—In this paper, we investigate the phenomenon of modulation instability (MI) and its associated gain spectra in Bragg grating (BG) structure for generating the ultrashort pulses. We analyze MI for the BG structure in fibers under the influence of non-Kerr nonlinearity. In addition, we also discuss the generation of BG solitons near the photonic bandgap in the BG structure from the induced MI gain spectra.**

***Index Terms*—Coupled-mode equation, fiber Bragg grating (BG), modulation instability (MI), soliton, ultrashort pulse.**

I. Introduction

The studies on modulational instability (MI) in both fiber and periodic structure in fiber known as fiber Bragg grating have attracted growing attention, in recent times, because of its fundamental and applied interests [1], [2]. One of the effects in fibers, known as MI, which occurs when a perturbed continuous wave experiences an instability that leads to an exponential growth of its amplitude or phase during the course of propagation in optical fibers due to an interplay between the nonlinearity and group velocity dispersion (GVD) act in opposition. That is, when the nonlinearity is positive GVD must be anomalous and if the nonlinearity is negative GVD must be normal. This is not applicable for different carrier frequencies of the interacting waves and for different directions of wave vectors. Note that the perturbation [of a continuous wave (CW)] can originate from quantum noise, the resulting MI is referred to as spontaneous MI, or from a frequency shifted signal, the resulting MI is known as induced MI. The occurrence of MI in fibers had been first suggested by Hasegawa and Brickman [3] and experimentally verified by Tai *et al.* [4]. MI has been observed for the first time for a single pump wave propagating in a standard non birefringent fiber and the resulting MI is called scalar MI. It is interesting to note that, in birefringent fiber the cross-phase modulation (XPM) between two modes extends the instability domain to the normal dispersion regime wherein the system involves more than one field component, which is in contrast to the result of a nonlinear Schrödinger (NLS) equation. This XPM induced MI is also called vector MI. In addition, various higher order linear and nonlinear effects such as higher dispersions, self-steepening, and time-delayed Raman effects have also been considered and these effects are found to strongly influence MI in fibers [1], [5]. MI is known to occur in many branches of physics like plasma physics, fluid dynamics and nonlinear optics. Among these branches, our intention is to investigate MI in nonlinear optics especially in fiber Bragg grating (FBG). For instance, in nonlinear optics this phenomena is important for the optical communication systems, the generation of short pulses with high repetition rates and the design of all-optical logical devices.

As happened in fiber, MI has also been investigated in FBG at low and high power levels for both anomalous and normal GVD regimes, corresponding to upper and lower branches of the dispersion curves [6]. In the anomalous GVD case, at relatively low powers, the gain spectrum is found to be similar as in the case of uniform index fiber. MI also occurs even in the normal GVD case where MI has threshold condition. In other words, the CW fields are unstable only when the power of CW fields exceeds the threshold condition [6]. In the later case, the instability is threshold less. Recently, MI has been observed experimentally in an apodized grating structure wherein a single pulse has been converted into a train of ultrashort pulses (USP) [7]. In addition to temporal instabilities, spatial temporal instabilities have also been studied in a nonlinear bulk medium with Bragg gratings in the presence of Kerr type nonlinearity [8]. Recently, in the dynamic grating, it has been experimentally shown that there is no power threshold for the occurrence of MI in the normal dispersion regime [9], [10]. More recently, we have also analyzed the occurrence of MI, the associated gain spectra and the generation of Bragg grating solitons from the MI gain spectra in the presence of Kerr nonlinearity [11].

In this paper, we discuss the necessary instability conditions and their associated gain spectra for generating USP near and away from the photonic bandgap (PBG) structure in FBG for non-Kerr media. This paper is organized as follows. In Section II, we discuss the necessary theoretical model for the pulse propagation in FBG. In Section III, we explore the characteristics of the nonlinear periodic structure through the nonlinear dispersion relations. To obtain the instability condition, we apply the (LSA) in Section IV. We present our discussion pertaining to MI gain spectra for non-Kerr media in Section IV. In Section V, we study the generation of Bragg grating solitons in the nonlinear periodic structure in the presence of quintic nonlinearity through the MI gain spectra. Finally, we present the conclusion of our work in Section VI.

Manuscript received September 14, 2004; revised December 17, 2004. The work of K. Porsezian was supported by the Department of Science and Technology, University Grants Commission (Research Award), Council of Science and Industrial Research, and the government of India through a research grant.

K. Porsezian and S. Devipriya are with the Department of Physics, Pondicherry University, Pondicherry 605 014, India (e-mail: ponzsol@yahoo.com; devipriya_ps@yahoo.co.in).

K. Senthilnathan is with the Department of Physics, Anna University, Chennai 600 025, India (e-mail: senthee2002@ yahoo.co.in).

Digital Object Identifier 10.1109/JQE.2005.847550

II. Theoretical Model

The interest for considering cubic–quintic (CQ) nonlinearity stems from the fact that a nonlinear correction to the medium's refractive index in the form $\delta n = n_2 I - n_4 I^2$, where I being the light intensity and the coefficients $n_2, n_4 > 0$ determine the nonlinear response of the media. Although, formally it may be obtained by an expansion of the saturable nonlinearity $\delta n = n_2 I \left[1 + (n_4/n_2) I\right]^{-1}$, it has handicap of being always self-focusing, $((d(\delta n))/dI) > 0$. However, the CQ model changes the sign of focusing at a critical intensity $I_c = (n_2/2n_4)$. An experimental measurement of the nonlinear dielectric response in the *para*-toluene salfonate (PTS) crystal aptly models the above-mentioned insights near 1600 nm [1]. The CQ nonlinearity can be achieved by doping a fiber with semiconductor materials. One should have positive sign $n_2^{(1)} > 0$ and large saturation intensity $I_{\rm sat}^{(1)}$. The other should have a negative sign $n_2^{(2)} < 0$ with nearly same magnitude and low saturation intensity i.e., $\left(I_{\rm sat}^{(2)} \ll I_{\rm sat}^{(1)}\right)$.

Furthermore, it is interesting to note that the Bragg grating-CQ model studied in this work is meaningful in both temporal and spatial domains. For the purpose of carrying out MI which serves as a precursor for generating a train of ultrashort pulses, we have analyzed our model in the temporal domain. However, the same equation applies to spatial domain i.e., a planar waveguide with BG structure which confirms the situation in the above-mentioned PTS crystal that gives rise to CQ nonlinearity. In the presence of quintic nonlinearity, the pulse propagation in a nonlinear periodic structure is governed by the NLCM equations of the form [12]

$$
\begin{aligned}
&i\frac{\partial E_f}{\partial z} + \frac{i}{v_g}\frac{\partial E_f}{\partial t} + \delta E_f + \kappa E_b + \alpha_1\left(\frac{1}{2}|E_f|^2 + |E_b|^2\right)E_f \\
&\quad - \alpha_2\left(\frac{1}{4}|E_f|^4 + \frac{3}{2}|E_f|^2|E_b|^2 + \frac{3}{4}|E_b|^4\right)E_f = 0 \\
&-i\frac{\partial E_b}{\partial z} + \frac{i}{v_g}\frac{\partial E_b}{\partial t} + \delta E_b + \kappa E_f + \alpha_1\left(\frac{1}{2}|E_b|^2 + |E_f|^2\right)E_b \\
&\quad - \alpha_2\left(\frac{1}{4}|E_b|^4 + \frac{3}{2}|E_f|^2|E_b|^2 + \frac{3}{4}|E_f|^4\right)E_b = 0
\end{aligned}
\tag{1}
$$

where z and t are the normalized spatial coordinate and time, and δ and κ are the detuning and linear coupling coefficients. The parameters α_1 and α_2 represent the cubic and quintic nonlinearity. For the first time, Atai *et al.* [12] introduced the quintic nonlinearity into the nonlinear coupled-mode (NLCM) equations and investigated two different families of zero-velocity solitons. Note that the set of (1) assume the usual ratio of 1:2 in front of the self-phase modulation (SPM) and XPM terms in the cubic nonlinear part [13], and the ratio 1:6:3 for the quintic nonlinear part [14]. More recently, Atai [15] carried out the interaction scenario of the Bragg grating solitons in the presence of quintic nonlinearity. However, to the best of our knowledge, the studies on the occurrence of MI under the influence of quintic nonlinearity have not been analyzed. Therefore, in this paper, we aim to obtain MI conditions and their associated gain spectra for generating ultrashort pulses near the PBG structure in the presence of quintic nonlinearity. Aforementioned CQ model is not only possible in nonlinear optics but also in plasma theory, condensed matter physics, nuclear physics, etc [1]. One more intriguing physical system, Bose–Einstein liquids can also be modeled by a quintic nonlinearity, though in a repulsive interaction.

III. Nonlinear Dispersion Relation

Before investigating the MI conditions, first we explore the characteristics of the nonlinear periodic structure in the presence of non-Kerr nonlinearity through the nonlinear dispersion relation. It has been well established that knowledge of the nonlinear dispersion curves obtained from the continuous wave solutions of the coupled-mode equations provide considerable physical insight into the existence of the photonic bandgap [2], [6]. Now, we discuss the derivation of nonlinear dispersion relation and analyze the role of nonlinearity on the PBG through the dispersion curves. In order to derive the nonlinear dispersion relation for the NLCM equations, we assume the following form of the solution

$$E_f = u_f e^{iqz} \qquad E_b = u_b e^{iqz} \tag{2}$$

where u_f and u_b are the amplitudes of the forward and backward waves along the grating length. Now, let us introduce a parameter $f = u_b/u_f$, which describes how the total power $P_0 = u_f^2 + u_b^2$ is divided between the forward and backward propagating waves. The amplitudes u_f and u_b can be written in terms of the total power as follows:

$$u_f = \sqrt{\frac{P_0}{1+f^2}} \qquad u_b = \sqrt{\frac{P_0}{1+f^2}}f. \tag{3}$$

Now, using (2) and (3) in (1), we obtain the following relations for q and δ:

$$q = -\frac{\kappa}{2f}(1-f^2) - \frac{\alpha_1 P_0}{4}\left(\frac{1-f^2}{1+f^2}\right) + \frac{\alpha_2 P_o^2}{4}\left(\frac{1-f^4}{(1+f^2)^2}\right) \tag{4a}$$

$$\delta = -\frac{\kappa}{2f}(1+f^2) - \frac{3\alpha_1 P_0}{4} + \frac{\alpha_2 P_0^2}{2}\left(1 + \frac{f^2}{(1+f^2)^2}\right). \tag{4b}$$

The above relation can be used to describe the role of nonlinearity on PBG structure. The parameter $f < 0$ represents (forward propagation) the upper branch of the dispersion curve where the grating induced dispersion is negative (anomalous GVD). Similarly, the parameter $f > 0$ corresponding to (backward propagation) the lower branch of the dispersion curve where the grating induced dispersion is positive (normal GVD). It is interesting to note that the parameter $f = \pm 1$ correspond to the two edges of the photonic bandgap where the grating exhibits significant higher order dispersion. The parameter $f = -1$ corresponds to the tuning the CW beam to the top of the bandgap and $f = 1$ corresponds to the tuning the CW beam to the bottom of the bandgap. In this paper, we are interested to investigate the occurrence of MI at the edges of PBG $(f = \pm 1)$ as well as on the upper $(f < 0)$ and lower $(f > 0)$ branches of the dispersion curve. In the forthcoming paragraph, we qualitatively discuss the impact of nonlinearity on PBG.

When we introduce the positive (negative) nonlinearity into the system, which increases (decreases) the average refractive index of the medium which in turn shifts the PBG such that the centre frequency does not fall within the frequency bandgap but corresponds to allowed band. It also means that the high intensity electric field shifts the PBG (i.e., central frequency) to either of upper or lower branches of the dispersion curves depending on the sign of nonlinearity. Thus positive nonlinearity shifts PBG down in energy and as a result the center frequency now locally tunes out of the gap i.e., to the upper edge of the PBG. Whereas negative nonlinearity shifts the PBG up in energy, meaning that the central frequency is now shifted toward the higher frequency side (to the lower edge of the PBG). When the power of this applied electric field exceeds the certain, say, threshold power i.e., critical power, the applied field drastically affects the PBG. Before embarking into the further discussion, we first calculate the critical power. This critical value of P_0 can be calculated by looking for the value of f at which q becomes zero while $f \neq 1$ from the nonlinear dispersion relation and is found to be

$$f \equiv f_c = -\frac{\left(\alpha_1 P_0 - \alpha_2 P_0^2\right)}{4\kappa} \pm \sqrt{\left(\frac{\alpha_1 P_0 - \alpha_2 P_0^2}{4\kappa}\right)^2 - 1}.$$

In order to study the role of quintic effect on the PBG structure, first we intend to study the physics behind the role of nonlinearity on PBG in the absence of quintic nonlinearity, which has been discussed in detail [2]. Whenever the applied input power P_0 exceeds the critical power, $P_C = (2\kappa/\alpha)$, there is a formation of loop on the upper branch of the dispersion curve which is clearly depicted in Fig. 1(a). For the negative nonlinearity, the loop is formed on the lower branch. From the literatures, it is known that the quintic effect can be treated either as self-focusing (SF) or self-defocusing (SDF) effect. However, nowadays, the researchers view the quintic effect as a SDF effect for achieving nearly ideal pulse propagation through the medium. Thus, the combination of the SF cubic and SDF quintic effects prevents collapse and hence one can anticipate the existence of stable solitons pulse propagation.

Therefore, we analyze both the SF and the SDF quintic effects on the dispersion curves. When we treat the quintic effect as SF effect, we find the size of the loop gets increased. On the other hand, when we treat the quintic effect as SDF effect, the size of the loop diminishes and eventually disappears when a large amount of negative nonlinearity (SDF) is introduced. This process is clearly shown in Fig. 1(b) and (c).

IV. Linear Stability Analysis

Now we turn to examine occurrence of MI in the nonlinear periodic structure through the LSA. The fundamental idea of LSA is to perturb the (system under consideration) CW solution slightly and then study whether this small perturbation grows or decays with propagation. It should be emphasized that LSA is valid as long as the perturbation amplitude remains small compared with the CW beam amplitude. In case, when the perturbation amplitude grows enough and if it is comparable to that of incident CW beam, then numerical analysis must be adopted. In this paper, we restrict to the former case. By following the standard procedure, we assume that solutions of the governing equations are perturbed slightly such that

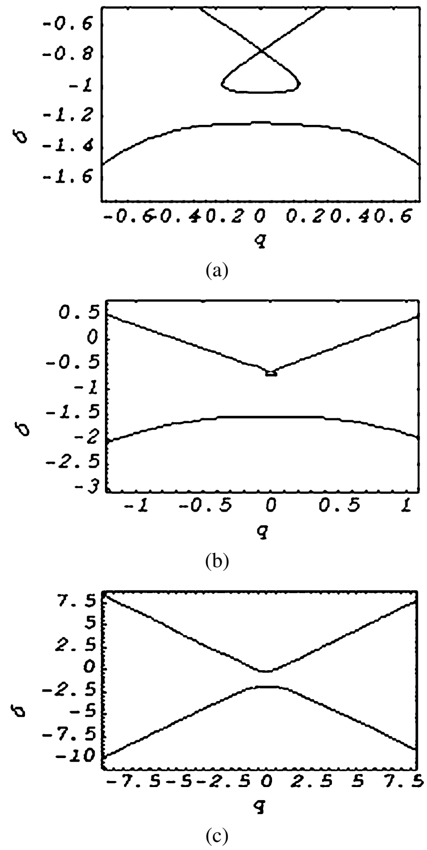

Fig. 1. (a) Role of negative nonlinearity on PBG. (b) Role negative nonlinearity on PBG when SDF $\alpha_2 = 0.4$. (c) Role negative nonlinearity on PBG when SDF $\alpha_2 = 0.9$.

$$A_j = (u_j + a_j) \exp(iqz), \quad j = f, b \tag{5}$$

with the perturbation $|a_j| \ll u$.That is,assuming the perturbation a_j is small, we substitute (5) to the basic equations and linearize in a_j to obtain

$$\begin{aligned} &i\frac{\partial a_f}{\partial z} + \frac{i}{v_g}\frac{\partial a_f}{\partial t} + \kappa a_b - \kappa f a_f \\ &\quad + \frac{\Gamma_1}{2}\left[\left(a_f + a_f^*\right) + 2f\left(a_b + a_b^*\right)\right] \\ &\quad - \Gamma_2\Bigg[\frac{1}{4}\left(a_f + 2a_f^*\right) + \frac{3}{2}f\left(a_b + a_b^*\right) + \frac{3}{2}f^2\left(a_f + a_f^*\right) \\ &\qquad + \frac{3}{2}f^3\left(a_b + a_b^*\right) + \frac{1}{2}f^4 a_f\Bigg] = 0 \end{aligned} \tag{6a}$$

$$\begin{aligned} &-i\frac{\partial a_b}{\partial z} + \frac{i}{v_g}\frac{\partial a_b}{\partial t} + \kappa a_f - \frac{\kappa}{f}a_b \\ &\quad + \frac{\Gamma_1}{2}\left[f^2\left(a_b + a_b^*\right) + 2f\left(a_f + a_f^*\right)\right] \\ &\quad - \Gamma_2\Bigg[\frac{3}{2}f\left(a_f + a_f^*\right) + \frac{3}{2}f^2\left(a_b + a_b^*\right) \\ &\qquad + \frac{3}{2}f^3\left(a_f + a_f^*\right) + \frac{1}{2}f^4\left(a_b + a_b^*\right)\Bigg] = 0 \end{aligned} \tag{6b}$$

where $\Gamma_1 = \left((\alpha_1 P_0)/(1+f^2)\right)$ and $\Gamma_2 = \left((\alpha_2 P_0^2)/\left((1+f^2)^2\right)\right)$. In order to solve the set of two linearized equations given by (6), we assume a plane wave ansatz constituting of both forward and backward propagation having the form [2], [6]

$$a_j = c_j \exp\left(i(Kz-\Omega t)\right) + d_j \exp\left(-i(Kz-\Omega t)\right) (j=f,b) \tag{7}$$

where c_j and d_j are real constants, K is the propagation constant and Ω is the perturbation frequency. Following the method discussed in [6], on substituting (7) to (6), we obtain a set of four linear coupled equations for c_j and d_j

$$\begin{aligned}&\left(-K+S-\kappa f+\frac{\Gamma_1}{2}-\frac{\Gamma_2}{4}-\frac{3}{2}\Gamma_2 f^2-\frac{\Gamma_2}{2}f^4\right)c_f\\&+\left(\kappa+\Gamma_1 f-\frac{3}{2}\Gamma_2 f-\frac{3}{2}\Gamma_2 f^3\right)c_b\\&+\left(\frac{\Gamma_1}{2}-\frac{\Gamma_2}{2}-\frac{3}{2}\Gamma_2 f^2\right)d_f\\&+\left(\Gamma_1 f-\frac{3}{2}\Gamma_2 f-\frac{3}{2}\Gamma_2 f^3\right)d_b=0\end{aligned} \tag{8a}$$

$$\begin{aligned}&\left(\kappa+\Gamma_1 f-\frac{3}{2}\Gamma_2 f-\frac{3}{2}\Gamma_2 f^3\right)c_f\\&+\left(K+S-\frac{\kappa}{f}+\frac{\Gamma_1}{2}f^2-\frac{3}{2}\Gamma_2 f^2-\frac{\Gamma_2}{2}f^4\right)c_b\\&+\left(\Gamma_1 f-\frac{3}{2}\Gamma_2 f-\frac{3}{2}\Gamma_2 f^3\right)d_f\\&+\left(\frac{\Gamma_1}{2}f^2-\frac{3}{2}\Gamma_2 f^2-\frac{\Gamma_2}{2}f^4\right)d_b=0\end{aligned} \tag{8b}$$

$$\begin{aligned}&\left(\frac{\Gamma_1}{2}-\frac{\Gamma_2}{2}-\frac{3}{2}\Gamma_2 f^2\right)c_f\\&+\left(\kappa+\Gamma_1 f-\frac{3}{2}\Gamma_2 f-\frac{3}{2}\Gamma_2 f^3\right)c_b\\&+\left(K-S-\kappa f+\frac{\Gamma_1}{2}-\frac{\Gamma_2}{4}-\frac{3}{2}\Gamma_2 f^2-\frac{\Gamma_2}{2}f^4\right)d_f\\&+\left(\kappa+\Gamma_1 f-\frac{3}{2}\Gamma_2 f-\frac{3}{2}\Gamma_2 f^3\right)d_b=0\end{aligned} \tag{8c}$$

$$\begin{aligned}&\left(\kappa+\Gamma_1 f-\frac{3}{2}\Gamma_2 f-\frac{3}{2}\Gamma_2 f^3\right)c_f\\&+\left(\frac{\Gamma_1}{2}f^2-\frac{3}{2}\Gamma_2 f^2-\frac{\Gamma_2}{2}f^4\right)c_b\\&+\left(\kappa+\Gamma_1 f-\frac{3}{2}\Gamma_2 f-\frac{3}{2}\Gamma_2 f^3\right)d_f\\&+\left(-K-S-\frac{\kappa}{f}+\frac{\Gamma_1}{2}f^2-\frac{3}{2}\Gamma_2 f^2-\frac{\Gamma_2}{2}f^4\right)d_b\\&=0.\end{aligned} \tag{8d}$$

This set has a nontrivial solution only when the 4×4 determinant formed by the coefficients matrix vanishes as given below

$$\begin{bmatrix} m_{11} & m_{12} & m_{13} & m_{14}\\ m_{21} & m_{22} & m_{23} & m_{24}\\ m_{31} & m_{32} & m_{33} & m_{34}\\ m_{41} & m_{42} & m_{43} & m_{44}\end{bmatrix}\begin{pmatrix}c_f\\c_b\\d_f\\d_b\end{pmatrix}=0$$

where

$$\begin{aligned}
m_{11} &= \left(-K+S-\kappa f+\frac{\Gamma_1}{2}-\frac{\Gamma_2}{4}-\frac{3}{2}\Gamma_2 f^2-\frac{\Gamma_2}{2}f^4\right)\\
m_{12} &= \left(\kappa+\Gamma_1 f-\frac{3}{2}\Gamma_2 f-\frac{3}{2}\Gamma_2 f^3\right)\\
m_{13} &= \left(\frac{\Gamma_1}{2}-\frac{\Gamma_2}{2}-\frac{3}{2}\Gamma_2 f^2\right)\\
m_{14} &= \left(\Gamma_1 f-\frac{3}{2}\Gamma_2 f-\frac{3}{2}\Gamma_2 f^3\right)\\
m_{21} &= \left(\kappa+\Gamma_1 f-\frac{3}{2}\Gamma_2 f-\frac{3}{2}\Gamma_2 f^3\right)\\
m_{22} &= \left(K+S-\frac{\kappa}{f}+\frac{\Gamma_1}{2}f^2-\frac{3}{2}\Gamma_2 f^2-\frac{\Gamma_2}{2}f^4\right)\\
m_{23} &= \left(\Gamma_1 f-\frac{3}{2}\Gamma_2 f-\frac{3}{2}\Gamma_2 f^3\right)\\
m_{24} &= \left(\frac{\Gamma_1}{2}f^2-\frac{3}{2}\Gamma_2 f^2-\frac{\Gamma_2}{2}f^4\right)\\
m_{31} &= \left(\frac{\Gamma_1}{2}-\frac{\Gamma_2}{2}-\frac{3}{2}\Gamma_2 f^2\right)\\
m_{32} &= \left(\kappa+\Gamma_1 f-\frac{3}{2}\Gamma_2 f-\frac{3}{2}\Gamma_2 f^3\right)\\
m_{33} &= \left(K-S-\kappa f+\frac{\Gamma_1}{2}-\frac{\Gamma_2}{4}-\frac{3}{2}\Gamma_2 f^2-\frac{\Gamma_2}{2}f^4\right)\\
m_{34} &= \left(\kappa+\Gamma_1 f-\frac{3}{2}\Gamma_2 f-\frac{3}{2}\Gamma_2 f^3\right)\\
m_{41} &= \left(\kappa+\Gamma_1 f-\frac{3}{2}\Gamma_2 f-\frac{3}{2}\Gamma_2 f^3\right)\\
m_{42} &= \left(\frac{\Gamma_1}{2}f^2-\frac{3}{2}\Gamma_2 f^2-\frac{\Gamma_2}{2}f^4\right)\\
m_{43} &= \left(\kappa+\Gamma_1 f-\frac{3}{2}\Gamma_2 f-\frac{3}{2}\Gamma_2 f^3\right)\\
m_{44} &= \left(-K-S-\frac{\kappa}{f}+\frac{\Gamma_1}{2}f^2-\frac{3}{2}\Gamma_2 f^2-\frac{\Gamma_2}{2}f^4\right).
\end{aligned}$$

This condition leads to a fourth-order polynomial in $S \equiv \Omega/v_g$ whose roots depend on K, κ, and P_0. The four roots of the polynomial in S so obtained determine the stability of the continuous wave solution. The above 4×4 matrix is referred to as stability matrix which is used to study the stability of the system under consideration. It is worth to note that the phenomenon of MI occurs only when at least one of the eigenvalues of the stability matrix possesses a nonzero and negative imaginary part that corresponds to an exponential growth of the amplitude of the perturbation. For the case of FBG, MI occurs when there is an exponential growth in the amplitude of the perturbed wave which implies the existence of a nonvanishing imaginary part in the complex parameter S [2], [6]. The MI phenomenon is measured by a gain given by $G \equiv |\mathrm{Im}\ S_m|$ where $\mathrm{Im}\ S_m$ denotes the imaginary part of S_m, where S_m is the root with the largest imaginary part.

In this paper, our aim is to investigate the occurrence of temporal (longitudinal) instabilities of two counter-propagating waves in a BG structure at the edges of the bandgap as well as on the upper and lower branches of the dispersion curve.

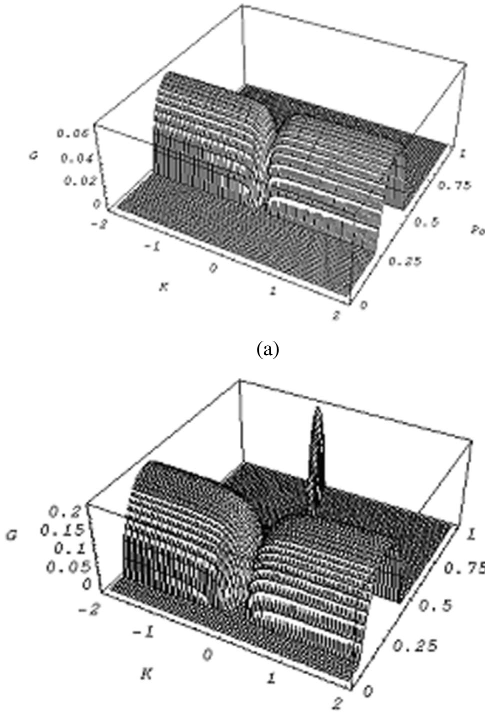

(a)

(b)

Fig. 2. (a). MI gain spectra in anomolous dispersion (AD) regime when $\kappa = 0.03, \alpha_1 = 0.05, \alpha_2 = 0.8, f = -2.5$. (b) MI gain spectra in AD regime when $\kappa = 0.03, \alpha_1 = 0.05, \alpha_2 = 0.01, f = -2.5$.

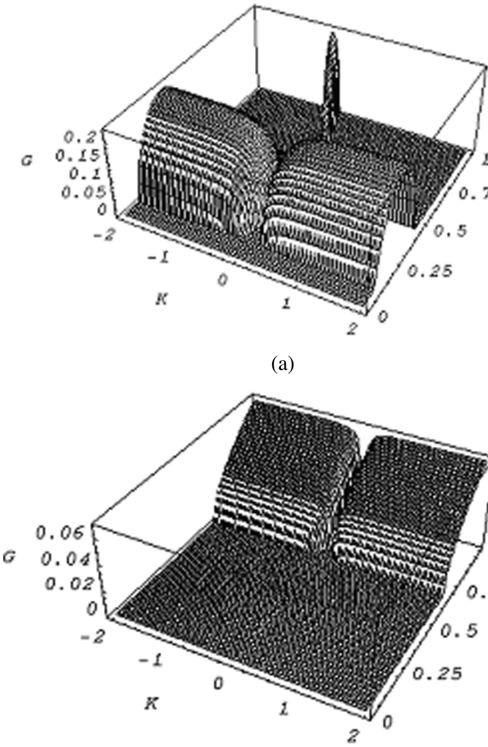

(a)

(b)

Fig. 3. (a).Top of PBG when $\kappa = 0.03, \alpha_1 = 0.05, \alpha_2 = 0.8, f = -1$. (b) Top of PBG when $\kappa = 0.03, \alpha_1 = 0.05, \alpha_2 = 0.1, f = -1$.

The results of this paper are presented in Sections IV-A–D. In first two subsections we discuss MI for the general case where ($f < 0$ *and* $f > 0$) the effects of detuning from the bandgap edges have been considered. Then we consider the two more special cases ($f = \pm 1$) for which the CW beam is exactly tuned to the top and the bottom of the photonic bandgap.

A. Anomalous Dispersion Regime ($f < 0$)

First we consider the general case where the parameter $f < 0$ describes the detuning of the CW from the edge of the PBG into upper branch of the dispersion curve where the grating induced dispersion is anomalous. We obtain the gain spectra of MI for both the anomalous and normal dispersion regimes for a particular value of the linear coupling constant κ i.e., $G(K, P_0) \equiv |\mathrm{Im}\, S_m(K, P_0)|$. We summarize the results obtained below.

To study the impact of quintic nonlinearity, initially we choose the small values of the physical parameters. For instance, we obtain the gain spectrum which is shown in Fig. 2(a) for comparatively small value of the quintic nonlinearity $\alpha_2 = 0.08$. As can be seen from Fig. 2(a), the maximum gain occurs at a nonzero value of P_0 and K. On the other hand, for comparatively large values of the quintic nonlinearity $\alpha_2 = 0.8$, the two centerlobes vanish and instead, we obtain a gain spectrum centered around the zero propagation constant region and having a maximum value along the line where the propagation constant vanishes as shown in Fig. 2(b) where the maximum gain occurs only at nonzero value of P_0, however the maximum gain occurs for the non zero value of the input power P_0. Also, the centered lobe broadens with increasing the value of the coupling parameter κ.

B. Top of the Photonic Bandgap ($f = -1$)

So far, we have considered the case for which $f < 0$. It is well known that the parameter $f = -1$ represents the tuning of the CW into the top of the photonic bandgap. Now on repeating the same procedure for $f = -1.0$, we observe that the gain spectrum is somewhat similar to anomalous dispersion case. This is clearly depicted in Fig. 3(a). From this figure, it is clear that the gain spectrum has a single peak in addition to the two distinct sidelobes. In this case also, the maximum gain occurs at a nonzero value of P_0 and K wherein the sidelobes have started to appear near $P_0 = 0.1$ whereas in the previous case the gain spectrum has started at $P_0 = 0.25$. As the quintic nonlinearity decreases, the sidelobes have been shifted toward the higher values of the input power $P_0 = 0.75$, which is clearly portrayed in Fig. 3(b). Note that the maximum gain still occurs for nonzero values of the propagation constant K and in put power P_0. However, the maximum gain decreases toward center where the propagation constant K has zero value. Similarly, the gain spectra tend to broaden as value of the coupling parameter increases.

C. Normal Dispersion Regime ($f > 0$)

Here consider another general case for which the parameter $f > 0$, which represents the detuning of the CW into the lower branch of the dispersion curve where the grating induced dispersion is normal (positive). The resulting gin spectrum in the normal dispersion regime has single curved shape whose gain increases along the propagation direction. Fig. 4(a) portrays the corresponding surface plot for the following physical parameter values of $\kappa = 1$ and $\alpha_2 = 0.2$. From this gain spectrum it is interesting to note that the maximum gain occurs at nonzero

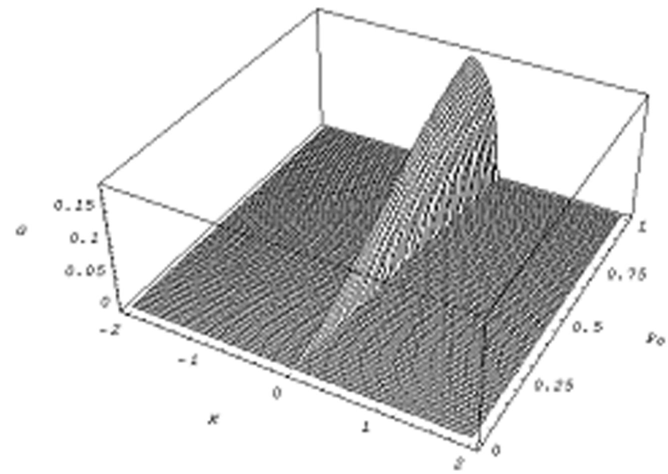

(a)

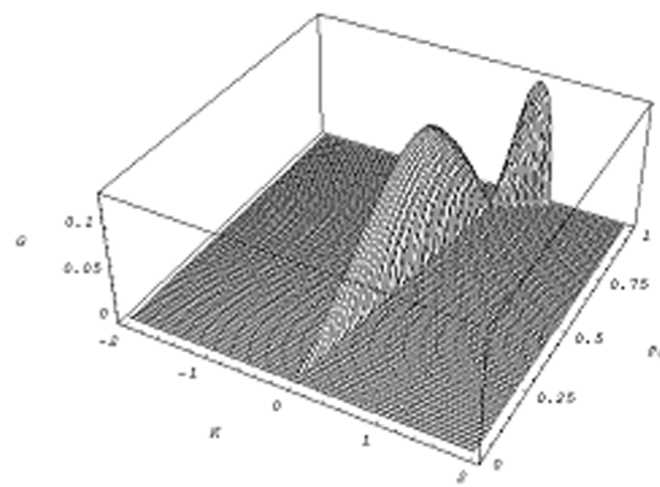

(b)

Fig. 4. (a) Normal dispersion (ND) regime when $\kappa = 1, \alpha_1 = 1, \alpha_2 = 0.8$, $f = 2.5$. (b) ND regime when $\kappa = 1, \alpha_1 = 1, \alpha_2 = 0.2, f = 2.5$.

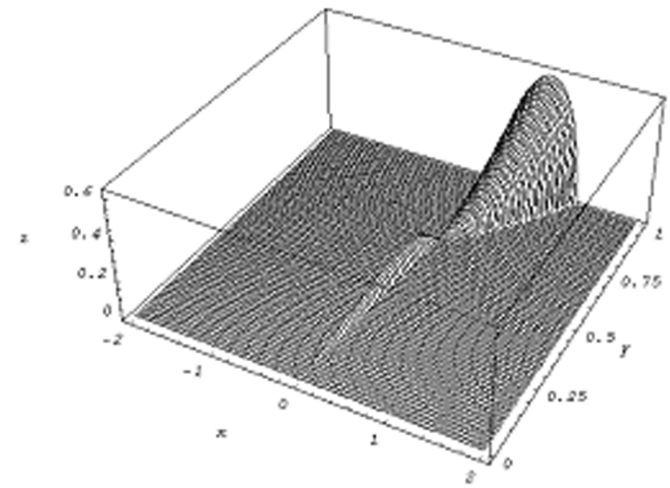

(a)

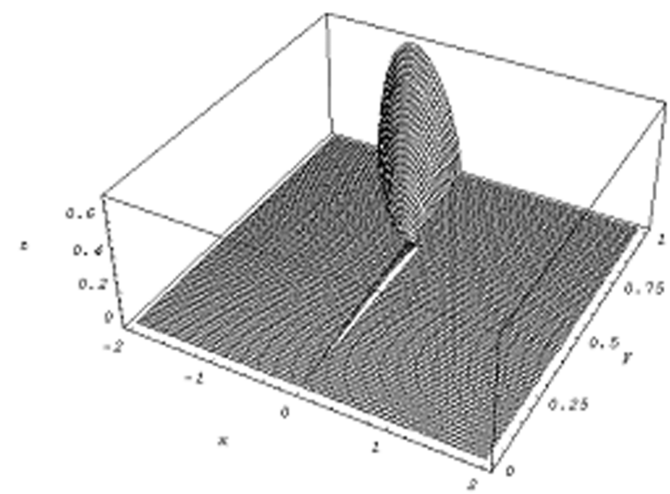

(b)

Fig. 5. (a). Bottom of PBG when $\kappa = 1, \alpha_1 = 1, \alpha_2 = 0.8, f = 1$. (b) Bottom of PBG when $\kappa = 1, \alpha_1 = 1, \alpha_2 = 0.6, f = 1$.

value of the propagation constant K. For comparatively large values of the quintic nonlinearity say $\alpha_2 = 0.8$, instead of single peak, the MI gain spectrum has two distinct peaks as depicted in Fig. 4(b). Note that the maximum gain decreases along the line where the propagation constant vanishes for which it has nil value.

D. Bottom of the Photonic Bandgap $(f = 1)$

As discussed earlier, $f = 1$ corresponds to tuning of the CW beam into the bottom of the photonic bandgap. On repeating the same procedure for $f = 1.0$, which depicts tuning at the bottom of PBG.

For comparatively large values of the quintic nonlinearity coefficient say $\alpha_2 = 0.8$, the gain spectrum has two distinct sidelobes wherein maximum gain of the first peak is less than the in the case of normal dispersion regime. The maximum gain occurs at both nonzero values of P_0 and K as depicted in Fig. 5(a). Another noteworthy point is that the amplitude of the first peak decreases as the quintic nonlinearity coefficient decreases. Fig. 5(b) explains the gain spectrum for comparatively low values of the quintic nonlinearity. From the figures, we observe that MI condition is achieved only for finite values of the input power. So far, we have plotted the gain spectrum by varying the input power P_0 and keeping linear coupling constant κ fixed. Therefore, one can pursue the above analysis and obtain gain spectrum by varying the linear coupling constant κ and keeping the input power P_0 fixed. This part will be discussed in the future publication.

Thus far, we have discussed MI under the influence of quintic nonlinearity. In what follows, we turn to point out the main differences between MI in this system compared to the MI in the Kerr medium. The MI in the Kerr medium differs from the non-Kerr medium mainly by the following factors: 1) MI gain spectra result within and near the PBG edges; 2) generated gap soliton from the MI gain spectra; and 3) peak power of the gap soliton results from the MI gain spectra. The influence of quintic nonlinearity can easily be understood by making the quintic effect equal to zero. The generation of gap solitons, in the presence of Kerr nonlinearity, through the MI analysis has been reported in the literature. Recently, for the nonlinearity management system, we have investigated the generation of gap solitons through the MI analysis under the influence of Kerr nonlinearity [11]. It is interesting to note that in the absence of non-Kerr nonlinearity, our results exactly concur with the earlier predicted results [11].

After the detailed analysis of the MI gain spectra for both anomalous and normal dispersion regimes in the upper and lower branches of the dispersion curve under the influence of non-Kerr nonlinearity, in Section V, we will discuss the existence of soliton in the upper branch of the dispersion curve through the same physical parameter values for which the MI gain spectra have already been obtained.

V. Generation of Solitons From Modulation Instability

In continuation of the occurrence of MI in both the dispersion regimes, now we proceed to discuss the existence of gap soliton in the upper branch of the dispersion curve through the MI gain spectra. Using multiple scale analysis, (1) has been reduced to the following form of the perturbed nonlinear Schrödinger (PNLS) equation:

$$i\frac{\partial E}{\partial z} + a\frac{\partial^2 E}{\partial t^2} + b|E|^2E + ic\frac{\partial^3 E}{\partial t^3} + id\left(|E|^2E\right)_t - e|E|^4E - if\left(|E|^4E\right)_t = 0. \quad (9)$$

Here, the variables are $\tau_1 = z$ and $Z = t$. In (9), the terms a, b, c, d, e, and f are the physical parameters of the NLCM equations in the nonlinear periodic structure. They are defined as follows: $a = (1/2\kappa)$, $b = ((3/2)\alpha_1)$, $c = (1/8\kappa^3)$, $d = (\alpha_1/4\kappa^2)$, $e = (5\alpha_2/4\kappa)$, $f = (\alpha_2/8\kappa^2)$. It is worth to note that the (9) describes the nonlinear pulse propagation in the upper branch of the dispersion curve under the influence of quintic nonlinearity. In (9), the variable 'E' represents the amplitude of the envelope associated with the Bloch wave formed by a superposition of E_f and E_b. Now, we discuss the generation of bright soliton near the PBG structure. As is well known, the effect of positive nonlinearity namely SF effect shifts the centre frequency of the optical pulse to the upper branch of the dispersion curve wherein the grating induces the anomalous dispersion. This SF effect and anomalous dispersion fight out to give birth to bright solitons near the PBG structure. Now we solve the (9) by the coupled amplitude-phase method. To start with, we consider the solution of the form

$$E(z,t) = Q(t+\beta z)\exp\left[i\left(kz - \omega t\right)\right] \quad (10)$$

where the function Q is a real one. The unknown parameters k and ω are directly related to the shifts in the wave number and frequency respectively. The factor β is the group velocity of the wave. The bright soliton in the upper branch under the influence of quintic nonlinearity is shown [16] in (11) at the bottom of the page, where $\chi = (t+\beta z)$, $\omega = ((c(b+e)+a(d+f))/(2c(d+f)))$, $k = (((a+3c\omega)/c)(2a\omega+3c\omega^2-\beta)-a\omega^2-c\omega^3)$. Equation (11) clearly shows the bright gap soliton profile in the presence of quintic nonlinearity in the upper branch of the dispersion curve. To realize the solitons (through MI analysis) from the experimental point of view, it is necessary to know the magnitude of the peak power to excite the gap soliton. Similarly, the soliton pulsewidth turns out to be another important physical parameter that is involved in the formation of a Bragg soliton. Based on the argument, we have also calculated the important and interesting physical parameters such as soliton power and pulsewidth and they are found to be

$$P_0 = \frac{2\left(2a\omega + 3c\omega^2 - \beta\right)}{\left(\frac{d}{2}\right) + \sqrt{\left(\frac{d}{2}\right)^2 - \frac{2}{3}\left(2a\omega + 3c\omega^2 - \beta\right)f}}$$

$$T_0 = \sqrt{\frac{1}{\left(2a\omega + 3b\omega^2 - \beta\right)}}.$$

One more intriguing physical parameter is the sample length which is required of the order of few centimeters to observe the above discussed effect. We hope that such estimates provide a valuable tool for determining the feasibility of experimental work. It should be noted that the existence of gap soliton in the upper branch of the dispersion curve has already been experimentally demonstrated in the Kerr medium [17]. However, the bright gap solitons in the non-Kerr media are yet to be experimentally investigated.

VI. Conclusion

In this paper, we have explored the characteristics of the nonlinear periodic structure in the presence of quintic nonlinearity through the nonlinear dispersion relation by studying the shift of the PBG in both upper and lower branches of the dispersion curve. From our investigation, we inferred that the introduction of the SF quintic nonlinearity in the system increases the size of the loop of the dispersion curve whereas SDF nonlinearity reduces the size of the loop. It can be noted that the further increment in the SDF nonlinearity leads to disappearance of the loop. It is mainly because of the fact that increasing the SDF nonlinearity minimizes the nonlinearity in the system. That is why the dispersion curves resemble the case of a PBG of a linear case. Based on the result, we come to the conclusion that SDF quintic nonlinearity acts as the nonlinearity management.

Secondly, we have investigated the modulational instability conditions required for the generation of ultrashort pulses in the nonlinear periodic structure under the influence of quintic nonlinearity for both the anomalous (upper branch) and normal dispersion (lower branch) regimes as well as at the edges of the photonic bandgap. We have also discussed the generation of bright gap soliton near the PBG structure in the nonlinear periodic structure in the presence of quintic nonlinearity. Besides, we have calculated the important and interesting physical parameters such as peak power and pulsewidth of the gap soliton which results from the MI gain spectra. We hope that such estimates provide

$$E(z,t) = \left[\frac{2\left(\frac{2a\omega+3c\omega^2-\beta}{c}\right)}{\left(\sqrt{\left(\frac{d}{2c}\right)^2 - \frac{2}{3}\left(\frac{2a\omega+3c\omega^2-\beta}{c^2}\right)f}\right)\cosh\left[2\sqrt{\left(\frac{2a\omega+3c\omega^2-\beta}{c}\right)}\chi\right] + \left(\frac{d}{2c}\right)}\right]^{1/2} e^{i(kz-\omega t)} \quad (11)$$

a valuable tool for determining the feasibility of experimental work. In this paper, our studies have been restricted to only temporal instabilities of two counter propagating waves. Therefore, it would be of great of interest to extend the above analysis to both longitudinal and transverse instabilities called spatiotemporal instability in a bulk medium having the grating structure.

REFERENCES

[1] Y. Kivshar and G. P. Agrawal, *Optical Solitons: From Fibers to Photonic Crystals*. San Diego, CA: Academic, 2003.

[2] G. P. Agrawal, *Applications of Nonlinear Fiber Optics*. San Diego, CA: Academic, 2001.

[3] A. Hasegawa and W. F. Brinkman, "Tunable coherent IR and FIR sources utilizing modulational instability," *IEEE J. Quantum Electron.*, vol. 16, no. 7, pp. 694–697, Jul. 1980.

[4] K. Tai, A. Hasegawa, and A. Tomita, "Observation of modulational instability in optical fibers," *Phys. Rev. Lett.*, vol. 56, pp. 135–138, 1986.

[5] R. Ganapathy and V. C. Kuriakose, "Cross-phase modulational instability in an elliptical birefringent fiber with higher order nonlinearity and dispersion," *Pramana J. Phys.*, vol. 58, pp. 669–684, 2002.

[6] C. M. de Sterke, "Theory of modulational instability in fiber Bragg gratings," *J. Opt. Soc. Amer. B*, vol. 15, pp. 2660–2667, 1998.

[7] B. J. Eggleton, C. M. de Sterke, A. B. Aceves, J. E. Sipe, T. A. Strasser, and R. E. Slusher, "Modulational instability and tunable multiple soliton generation in apodized fiber gratings," *Opt. Comm.*, vol. 149, pp. 267–271, 1998.

[8] N. M. Lichinitser, C. J. McKinstrie, C. M. de Sterke, and G. P. Agrawal, "Spatiotemporal instabilities in nonlinear bulk media with Bragg gratings," *J. Opt. Soc. Amer. B*, vol. 18, pp. 45–54, 2001.

[9] S. Pitios, M. Haelterman, and G. Millot, "Bragg modulational instability induced by a dynamic grating in an optical fiber," *Opt. Lett.*, vol. 26, pp. 780–782, 2001.

[10] ——, "Theoretical and experimental study of Bragg modulational instability in a dynamic fiber grating," *J. Opt. Soc. Amer. B*, vol. 19, pp. 782–791, 2002.

[11] R. Ganapthy, K. Senthilnathan, and K. Porsezian, "Modulational instability in a fiber and a fiber Bragg grating," *J. Opt. B, Quantum Semiclass. Opt.*, vol. 6, pp. S436–452, 2004.

[12] J. Atai and B. A. Malomed, "Families of Bragg-grating solitons in a cubic-quintic medium," *Phys. Lett. A*, vol. 284, pp. 247–252, 2001.

[13] G. P. Agrawal, *Nonlinear Fiber Optics*. San Diego, CA: Academic, 2001.

[14] A. I. Maimistov, B. A. Malomed, and A. Desyatnikov, "A potential of incoherent attraction between multidimensional solitons," *Phys. Lett. A*, vol. 254, pp. 179–184, 1999.

[15] J. Atai, "Interaction of Bragg-grating solitons in a cubic-quintic medium," *J. Opt. B. Quantum Semiclass. Opt.*, vol. 6, pp. S177–181, 2004.

[16] K. Senthilnathan, P. R. Babu, K. Porsezian, V. Santhanam, and S. Gnanasekaran, "Grating solitons near the photonic bandgap of a fiber Bragg grating," *J. Lightw. Technol.*, submitted for publication.

[17] B. J. Eggleton, R. E. Slusher, C. M. de Sterke, P. A. Krug, and J. E. Sipe, "Bragg grating solitons," *Phys. Rev. Lett.*, vol. 76, pp. 1627–1630, 1996.

K. Porsezian was born in Gudiyattam, India, on June 5, 1963. He received the M.Sc. degree from the University of Madras, India, in 1985 and the Ph.D. degree from Bhrathidasan University, Tiruchirapalli, India, in 1991.

At present, he is working as a Reader in the Raman School of Physics, Pondicherry University, Pondicherry, India. He has published approximately 70 papers and edited two books on optical solitons. His research interests are nonlinear fiber optics, SIT solitons, integrability aspects of nonlinear physical systems, and beam propagation in photorefractive media.

Dr. Porsezian is a recipient of the UGC Research Award (2004–2007), the Sathya Murthy Memorial Award for the Year 1997, given by the Indian Physics Association (1998), the Anil Kumar Bose Memorial Award given by the INSA (1998), the DAAD Post Doctoral Fellow (1995–1997), the AssociateshipAward from the ICTP, Italy (1997–2004), the AICTE Career Award for Young Teachers (1998–2000), the Indian National Science AcademyYoung Scientist Medal (1995), and the Junior Associateship Award from the ICTP, Italy (1995–1997).

K. Senthilnathan was born in Kattukkanallur, India, on June 12, 1977. He received the M.Sc. and M.Phil. degrees in physics from the University of Madras, Madras, India. He was awarded gold medal for his M.Phil degree. He received the Ph.D. degree from Anna University, Chenia, India.

His primary research interests are based on studying the linear and nonlinear properties of fiber and fiber Bragg gratings, nonlinear waveguides, and beam propagation in photorefractive media.

S. Devipriya was born in Anaikarai, India, on November 8, 1980. She received the M.Sc. degree in physics from Pondicherry University, Pondicherry, India, where she is currently working toward the M.Phil. degree.

Her primary research interests are based on studying the linear and nonlinear properties of fiber and fiber Bragg gratings.